IEEE Access
Multidisciplinary | Rapid Review | Open Access Journal

Received May 29, 2017, accepted June 6, 2017, date of publication June 16, 2017, date of current version July 7, 2017.

Digital Object Identifier 10.1109/ACCESS.2017.2716344

An Autonomous Wireless Body Area Network Implementation Towards IoT Connected Healthcare Applications

TAIYANG WU, (Student Member, IEEE), FAN WU, (Student Member, IEEE), JEAN-MICHEL REDOUTÉ, (Senior Member, IEEE), AND MEHMET RASIT YUCE, (Senior Member, IEEE)

Department of Electrical and Computer Systems Engineering, Monash University, Melbourne, VIC 3800, Australia

Corresponding author: Taiyang Wu (taiyang.wu@monash.edu)

The work of M. R. Yuce was supported by Australian Research Council Future Fellowships under Grant FT130100430.

ABSTRACT Internet of Things (IoT) is a new technological paradigm that can connect things from various fields through the Internet. For the IoT connected healthcare applications, the wireless body area network (WBAN) is gaining popularity as wearable devices spring into the market. This paper proposes a wearable sensor node with solar energy harvesting and Bluetooth low energy transmission that enables the implementation of an autonomous WBAN. Multiple sensor nodes can be deployed on different positions of the body to measure the subject's body temperature distribution, heartbeat, and detect falls. A web-based smartphone application is also developed for displaying the sensor data and fall notification. To extend the lifetime of the wearable sensor node, a flexible solar energy harvester with an output-based maximum power point tracking technique is used to power the sensor node. Experimental results show that the wearable sensor node works well when powered by the solar energy harvester. The autonomous 24 h operation is achieved with the experimental results. The proposed system with solar energy harvesting demonstrates that long-term continuous medical monitoring based on WBAN is possible provided that the subject stays outside for a short period of time in a day.

INDEX TERMS Internet of Things, wireless body area network, energy harvesting, maximum power point tracking, Bluetooth.

I. INTRODUCTION

Internet of Things (IoT) is a new technological paradigm that gains attention from vast research fields in the past few years [1], [2]. In the future healthcare circumstance, the IoT will connect the subjects and the healthcare professionals seamlessly [3], [4]. With the advancement of wearable sensors, low-power integrated circuit (IC) and wireless communication technologies, the wireless body area network (WBAN) is becoming an emerging research field worldwide [5]. WBAN, also known as body sensor network (BSN), is a wireless network to enable the health monitoring anywhere anytime around the human body [6], [7]. This can be used for the e-health applications, such as the computer-assisted rehabilitation, early detection of medical issues and emergency notification [8]. In recent years, the portable devices, especially smartphones, have almost been an indispensable part of people's daily life. Therefore, they can be employed as the gateway between the WBAN and the IoT cloud [9]–[11], as shown in Fig. 1.

Wearable sensors are the key components in the WBAN as they collect the vital data of the human body for further usage. Researchers from multiple disciplines have presented different wearable sensor systems for the WBAN applications. In [12], the authors present a wearable photoplethysmography (PPG) sensor for the heartbeat measurement at the earlobe. Another heartbeat sensor is presented in [13], which is designed with the polymer-based flexible strain-gauge sensor. A wearable sensor prototype capable of measuring heart rate, blood oxygen saturation, temperature and humidity during a magnetic resonance imaging (MRI) experiment is presented in [14]. Seeger *et al.* propose a middleware solution for the wearable sensor system of WBAN, which is based on the smartphone applications [15].

Another critical issue in the development of WBAN is the power consumption in the long-term use of wearable devices. Energy harvesting, especially wearable energy harvesting technology, is a promising solution to enable the long-term operation of WBAN [16]. In [17], the authors present

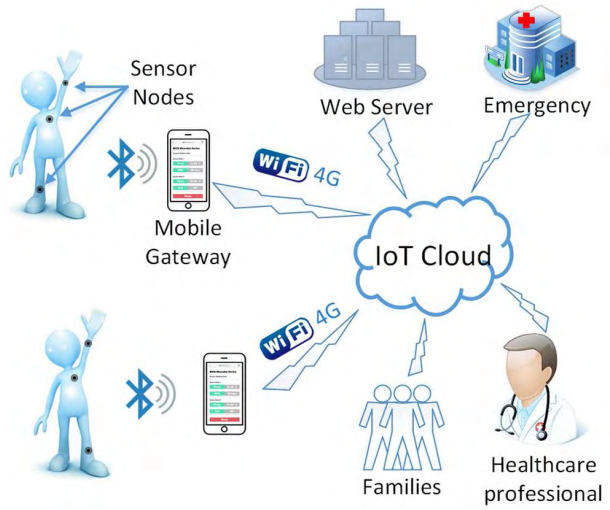

FIGURE 1. Wireless body area network with IoT connected healthcare platform.

a flexible energy harvesting mechanism for ultra-low power wearable devices. It also studies the performance of a flexible solar panel under different irradiance levels. Hamid and Yuce present a novel wearable energy harvester that combines piezoelectric and electromagnetic energy sources from low frequency vibrations like human motion [18]. In [19], a wearable bracelet with ultra-low power camera and microphone is presented. It is powered by hybrid solar cells and thermoelectric generators (TEGs), and its self-sustainability is confirmed by simulations based on experimental measurements. In [20], an autonomous wearable system with energy harvesting module is designed, manufactured and tested for vital signs measurement. The wearable system powered by a flexible solar panel can be attached to a T-shirt. Another optimal energy harvester using a flexible photovoltaic module and a maximum power point tracking (MPPT) technique based on fuzzy logic is proposed in [21]. It is used to power a sensor node with bluetooth low energy (BLE) module, which can measure heartbeat and blood pressure of the subject and send them to a smartphone.

This paper proposes a wearable sensor node with solar energy harvesting and BLE transmission to implement an autonomous WBAN. The solar energy harvester is controlled by an output based MPPT technique to extract the maximum power from a flexible solar panel [22]. The sensor node is integrated with an onboard accelerometer, temperature sensor and a plug-in PPG sensor on a flexible solar panel. Multiple nodes can be deployed on different positions of the body to measure the temperature distribution of the body. The node can also measure the heartbeat and detect the fall of the subject. All the data from the sensor nodes and fall notification will be transmitted to a web-based smartphone application through a commercial BLE module. When the sensor node is set to an appropriate wake-sleep mode, the 24 hours operation of the sensor node powered by the solar energy harvester is achieved and verified by experiments.

The remainder of the paper is organized as follows: Section II describes the system architecture. The solar energy harvester with the output based MPPT technique is presented in Section III. Section IV shows the experimental results of the solar energy harvester and the wearable sensor node. Lastly, the paper is concluded with a discussion of future improvement in Section V.

II. SYSTEM ARCHITECTURE

This paper presents the implementation of an autonomous WBAN towards the IoT connected healthcare applications. It consists of 3 major parts: 1) a flexible solar energy harvester with MPPT; 2) a wearable sensor node with BLE transmission; and 3) a smart phone application acting as the IoT gateway for sensor data visualization and emergency notification. Fig. 2 shows the overview of the wearable sensor node with solar energy harvesting.

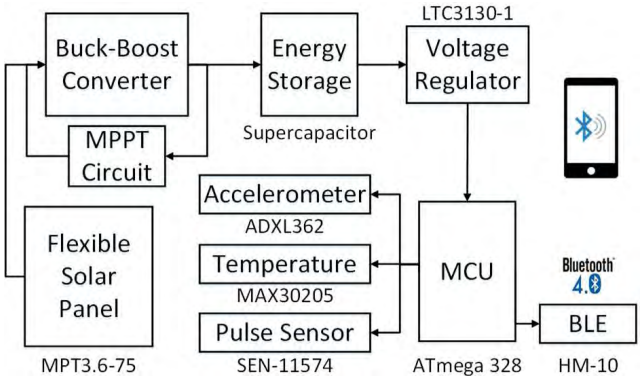

FIGURE 2. Flexible wearable sensor node with energy harvesting.

A. FLEXIBLE SOLAR ENERGY HARVESTER

A flexible solar panel, the MPT3.6-75 from Sundance Solar® (7.2*6.0 cm^2), is chosen as the power source for the energy harvester. Due to its flexibility, it can be easily attached to the human body for wearable applications. To extract the maximum power from the flexible solar panel, an output based analog MPPT circuit is proposed, which will be explained in detail in Section III. The harvested energy from the flexible solar panel is stored in a supercapacitor. Here a supercapacitor is chosen instead of a rechargeable battery. Because a supercapacitor has almost unlimited charging cycles, and its efficiency of charging and discharging is higher than that of a battery [23]. An efficient buck-boost voltage regulator, the LTC3130-1 from Linear Technology®, is adopted to connect the supercapacitor with the wearable sensor node. The input range of the voltage regulator is from 2.4 V to 25 V, and its output voltage is configured at 3.3 V to power the wearable sensor node.

B. WEARABLE SENSOR NODE

The main components of the wearable sensor node include a microcontroller unit (MCU) and 3 sensors for subject data

measurement and processing. The software diagram of the wearable sensor node is illustrated in Fig. 3.

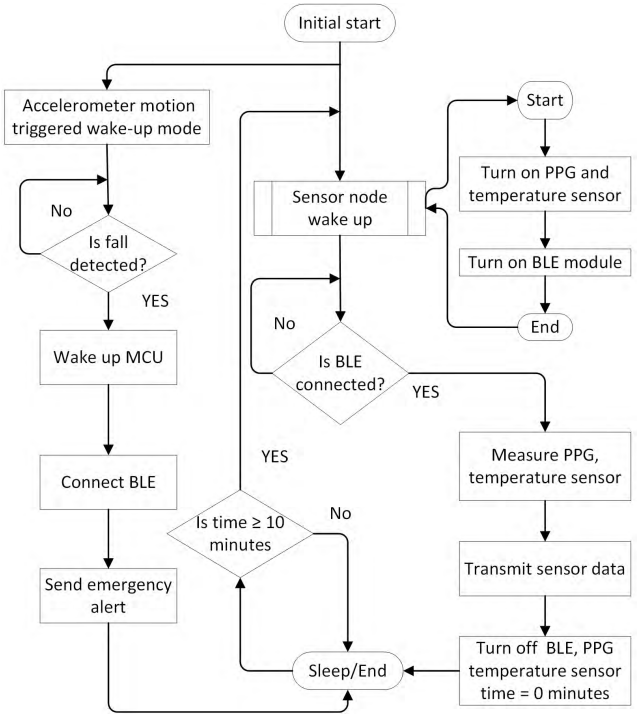

FIGURE 3. Software diagram of the wearable sensor node.

1) MCU

The core of the wearable sensor node is the MCU, which is used to collect and process the sensor data, as well as perform power management to reduce the overall power consumption. The MCU used in the sensor node is the ATmega328P from Atmel® due to its low power, low cost and high performance. The CPU speed of the MCU is configured to 8 MHz at 3.3 V, and it can be throttled down to 1 MHz at 1.8 V for extremely low power applications. The MCU has 32 KB flash memory with 2 KB SRAM, 6 analog input pins and 14 digital I/O pins. Therefore, the proposed wearable sensor node can be connected with other plug-in sensors such as ECG, EEG and GSR for other human body vital signals measurement in the future designs.

2) ACCELEROMETER

The ADXL362 from Analog Devices® is selected and soldered on the flexible PCB in the wearable sensor node. It is a 3-axis MEMS accelerometer with ultralow power consumption, which consumes less than 2 μA when the output data rate is 100 Hz and only 270 nA when it is in the motion triggered wake-up mode. The motion triggered wake-up mode is one of the most notable features of the accelerometer, and it has adjustable threshold of the sleep/wake motion activation. In the proposed wearable sensor node, the ADXL362 accelerometer is used for ''fall detection'' in the WBAN applications. Whenever a fall is detected, the ADXL362 wakes the MCU up and an emergency notification will be sent to the smartphone of the medical assistant through the BLE module.

3) TEMPERATURE SENSOR

The second onboard sensor is a temperature sensor, the MAX30205 from Maxim®. It is chosen due to its high accuracy (0.1°C from 37°C to 39°C), high resolution (16-bit) and low power consumption (600 μA at 2.7 V to 3.3 V). The MAX30205 temperature sensor can also provide an overtemperature alarm and communicate with the MCU through an I^2C-compatible 2-wire serial interface. The temperature sensor measures the body temperature distribution when the wearable sensor node is placed at different positions of the body.

4) PULSE SENSOR

A commercial pulse sensor is adopted in the wearable sensor node for subject heartbeat monitoring. The pulse sensor is a plug-in PPG sensor, which is only connected to the sensor node deployed at the subject's wrist. The pulse sensor consists of the low power light photo sensor (APDS-9008) and amplifier (MCP6001) with the typical supply current of 42 μA and 100 μA, respectively. By appropriate configuration, the pulse sensor can measure the heartbeat of the radial artery at the wrist instead of the fingertip, thus it will not interfere with the subject's daily life.

C. BLE TRANSMISSION AND SMARTPHONE APPLICATION

To help the medical assistant in analysing the data from the wearable sensor node, a BLE module (HM-10) is used to transmit the sensor data of the subject to a smartphone. The BLE module incorporates CC2541 chip from Texas Instrument®, which is a bluetooth low energy compliant and proprietary RF system-on-chip. The CC2541 is highly suited for low power consumptions as its RX and TX currents are 17.96 mA and 18.2 mA respectively. The BLE module can communicate with most of the iOS and Android smartphones with Bluetooth 4.0 on the market. For the sensor data visualization, a web-based smartphone application using the Evothings® platform is developed. The Evothings is a platform that enables wrapping up the CSS, HTML5 and Javascript code depending upon the device platform, instead of relying on the platform-specific APIs in the Android or iOS systems. Every smartphone with the Evothings Viewer application installed can access the sensor data through the designed application. This will help the medical assistant or family member monitor the subject's health conditions continuously.

Fig. 4 shows the PCB design for the wearable sensor node with the energy harvesting and the MPPT circuit (5.0*4.8 cm^2). The sensor circuit is fabricated with a flexible PCB, together with the flexible solar panel, the node is wearable and can be attached to the subject easily.

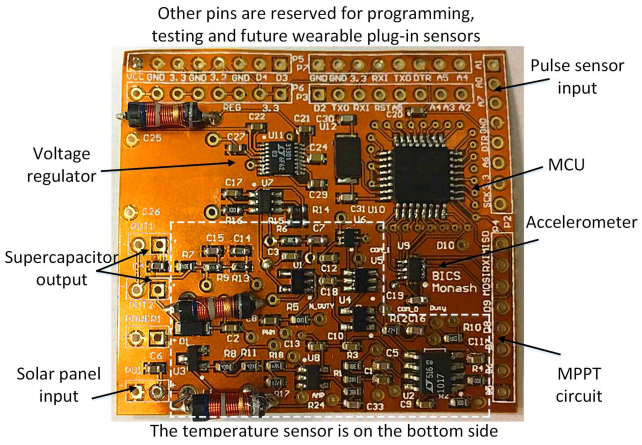

FIGURE 4. Flexible PCB design for the wearable sensor node circuit with MPPT (5.0*4.8 cm^2).

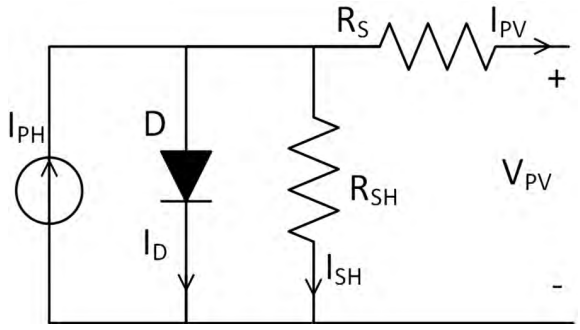

FIGURE 5. The electrical equivalent circuit of a solar panel.

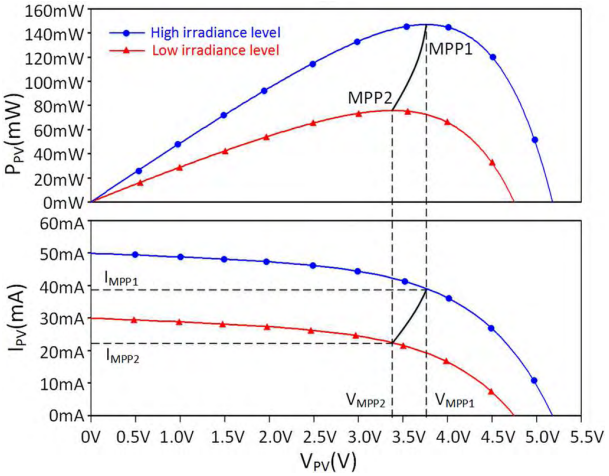

FIGURE 6. I-V and P-V characteristics of a solar panel under different irradiance levels.

III. SOLAR ENERGY HARVESTER WITH MPPT

A. SOLAR PANEL AND MPPT

A solar panel, also known as a photovoltaic (PV) module, is a nonlinear semiconductor device that absorbs the energy of the light and converts it into electricity. The electrical energy generated by the solar panel varies with the environmental conditions. An electrical equivalent circuit model of the solar panel is proposed in [24], as shown in Fig. 5. The current-voltage (I-V) characteristic of the solar panel can be given by:

$$I_{PV} = I_{PH} - I_0\left(e^{\frac{q(V_{PV}+I_{PV}R_S)}{\eta kT}} - 1\right) - \frac{V_{PV} + I_{PV}R_S}{R_{SH}} \quad (1)$$

where I_{PH} is the photo current, I_0 is the dark saturation current of the diode, q is the electronic charge, η is the ideality factor of the diode, k is the Boltzmann's constant and T is the temperature in Kelvin.

According to (1), the I_{PV} and V_{PV}, as well as the corresponding power (P_{PV}) of the solar panel , depend on the light irradiance level (I_{PH}) and temperature (T). Fig. 6 shows the I-V and P-V characteristics of a solar panel under different irradiance levels. It can be seen that the solar panel can output the maximum power at a certain point, which is called the maximum power point (MPP). However, the MPP moves due to the variation of the irradiance level and other environmental conditions. Therefore, to harvest the maximum power from a solar panel, the MPPT circuit is usually adopted within the power management unit in a solar energy harvesting system.

So far, there have been a lot of studies on the maximum power point tracking techniques for the application of solar energy harvesting [25], [26]. One of the most commonly used MPPT techniques is the perturbation and observation (P&O) [27], which is an iterative method to reach the MPP of a solar panel. It measures both the voltage and current to calculate the power of the solar panel and perturbs the operating point by changing the duty cycle of the DC-DC converter used in the solar energy harvester periodically. If the power from the solar panel increases, the P&O will keep the change of the duty cycle in the same direction; otherwise, it will change the duty cycle in the opposite direction. Eventually the duty cycle will oscillate around a value corresponding to the MPP, where the solar panel can output the maximum power. The implementation of the P&O technique is complex as it needs both the voltage and current to calculate the power [28]. Another common MPPT technique is the fractional open circuit voltage (FOCV) technique [29], which assumes the voltage at the MPP is proportional to the open circuit voltage of the solar panel. It simplifies the implementation of the MPPT circuit as only the voltage is required for the measurement. The limitation of FOCV is that the proportion of the voltage at the MPP to the open circuit voltage is based on the experimental observation. The proportion varies with the irradiance level and temperature, which means the tracking of MPP is not always precise. There are also other MPPT techniques, like the incremental conductance (IC), short circuit current (SCC) and temperature based MPPT technique [25]. With the improvement of microcontroller processing power, researchers have proposed more intelligent MPPT techniques, like the fuzzy logic control (FLC) and the neural network technique [26].

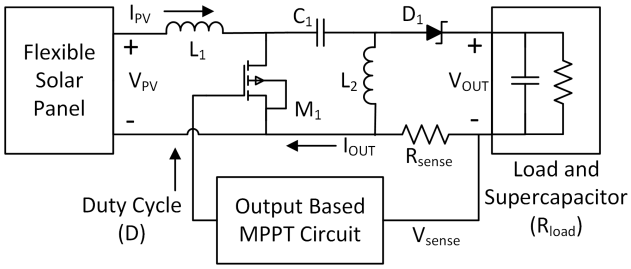

FIGURE 7. Block diagram of the flexible solar energy harvester.

B. PROPOSED OUTPUT BASED MPPT TECHNIQUE

In this work, the wearable sensor node is powered by a flexible solar energy harvester, whose block diagram is shown in Fig. 7. The flexible solar panel and the load is connected by a buck-boost converter, consisting of L_1, L_2, C_1 and M_1. To harvest the maximum power from the solar panel, an output based MPPT technique is proposed to control the duty cycle (D) of the buck-boost converter for impedance matching [30].

For the buck-boost converter, the relationship of the input (V_{PV} & I_{PV}) and output (V_{OUT} & I_{OUT}) can be expressed as:

$$V_{PV} = \frac{1-D}{D} V_{OUT} \tag{2}$$

and

$$I_{PV} = \frac{D}{1-D} I_{OUT} \tag{3}$$

Thus the equivalent resistance of the output load seen from the input side of the buck-boost converter is:

$$R_{eq} = \frac{(1-D)^2}{D^2} R_{load} \tag{4}$$

From the I-V characteristic of the solar panel in Fig. 6, there exists a resistance ($R_{MPP} = V_{MPP}/I_{MPP}$) corresponding to the MPP. This means the solar panel can output the maximum power when the load resistance equals R_{MPP}. By changing the D in (4), the equivalent resistance R_{eq} can be matched to the R_{MPP}, therefore the MPP of the solar panel is reached.

To measure the power of the solar panel, conventional MPPT techniques (like P&O) multiply the V_{PV} and I_{PV} at the input side of the DC-DC converter. The proposed MPPT technique focuses on the output side and only needs one parameter. For a constant resistive load (R_{load}) at the output side, the output power is:

$$P_{OUT} = I_{OUT}^2 R_{load} \tag{5}$$

Considering the efficiency η of the buck-boost converter, the input power from the solar panel is:

$$P_{PV} = \frac{I_{OUT}^2 R_{load}}{\eta} \tag{6}$$

According to (6), the power of the solar panel has the same changing trend of the output current I_{OUT}. The proposed MPPT measures the I_{OUT}, and then changes the (D) of the buck-boost converter (increase). If the measured I_{OUT} also increases, the MPPT circuit will keep changing D in the same direction (increase); otherwise the MPPT circuit will change D in the opposite direction (decrease). Through this method, the D will be fixed around a certain value while the I_{OUT} is maximum, which means the power of the solar panel is also maximum. For a variable load or supercapacitor, the above analysis can still be applicable. As in a short period time, the variable load or the supercapacitor can be treated like a fixed load. As long as the variation of the load or supercapacitor is within the tracking time of the MPPT circuit, the solar panel will operate around its MPP and output the maximum power.

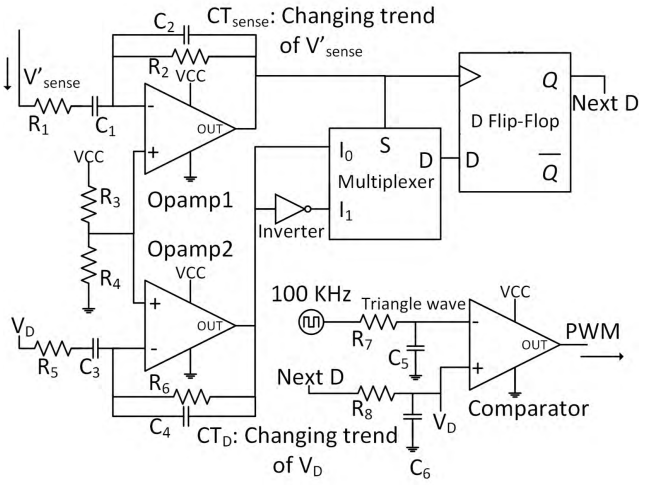

FIGURE 8. Circuit design of the output based MPPT technique.

The implementation of the proposed MPPT circuit is shown in Fig. 8. The I_{OUT} is sensed by a small resistor R_{sense} (in Fig. 7), thus I_{OUT} can be represented by V_{sense}, which is amplified to V'_{sense} for accurate processing. V'_{sense} is the input of the first differentiator, which consists of $Opamp1, R_1, R_2, C_1$ & C_2. The output of the differentiator indicates the changing trend of V'_{sense}: the CT_{sense} is low when V'_{sense} increases and CT_{sense} is high when V'_{sense} decreases. The second differentiator consisting of $Opamp2, R_5, R_6, C_3$ & C_4 has the similar configuration and is used to detect the changing trend of V_D (CT_D). V_D is the voltage of C_6, and it is compared with a triangle wave generated by a 100 KHz clock, R_7 & C_5. The comparison result is the final output of the MPPT circuit, which is a PWM signal used to drive the buck-boost converter. Because V_D is proportional to the duty cycle value of the PWM signal, its changing trend CT_D represents the changing trend of the duty cycle.

The changing trend of the I_{OUT} and D, which are denoted by CT_{sense} and CT_D respectively, are used to track the MPP of the solar panel. The simulation result of the tracking process by LTspice® is illustrated in Fig. 9. The CT_{sense} is the control signal input of the multiplexer and the rising edge D flip-flop. The CT_D and its inverted value are the inputs of the

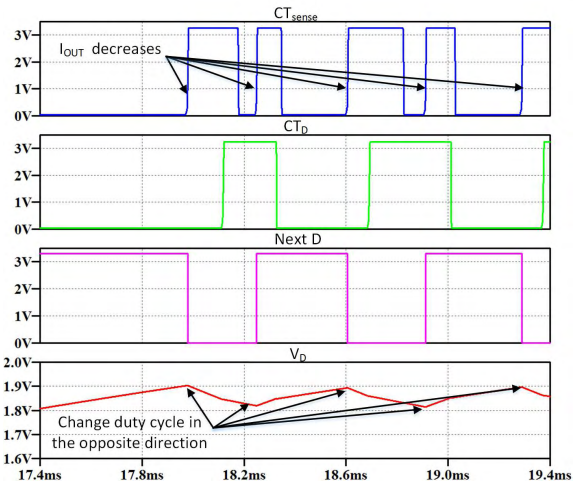

FIGURE 9. Tracking process of the output based MPPT technique.

multiplexer. The output of the multiplexer is the input of the D flip-flop. The output of the D flip-flop, *Next D*, is used to charge or discharge C_6, which changes the duty cycle of the PWM signal. When the I_{OUT} increases, the CT_{sense} is low thus the output of the D flip-flop (*Next D*) will not change. The change of the duty cycle will be kept in the same direction (increase/decrease). When the I_{OUT} decreases, the CT_{sense} is changed to high. The multiplexer will output the inverted value of the changing trend of the duty cycle to the D flip-flop, thus the D flip-flop changes its output *Next D*. Then the duty cycle will be changed in the opposite direction (decrease/increase) to track the MPP of the solar panel. This tracking process will continue to control the solar panel to operate around its MPP. Note there are delays in the detection of the I_{OUT} and V_D, therefore the D flip-flop with rising edge is used in the tracking process.

IV. EXPERIMENTAL RESULTS

A. FLEXIBLE SOLAR ENERGY HARVESTER

The solar energy harvester with the output based MPPT is fabricated and tested with a flexible solar panel. To validate the performance of the proposed MPPT circuit, the characteristics of the flexible solar panel under different weather conditions are measured and shown in Fig. 10. The ''direct sunlight'' indicates that the solar panel is exposed to sunlight directly, while ''artificial shadow'' means using a paper board to block the direct sunlight to simulate the cloudy weather. The MPP of the flexible solar panel occurs around 3 V and 2.5 V under the direct sunlight and artificial shadow, respectively. Fig. 11 shows the experimental result of charging a 12.5 F supercapacitor with rate voltage of 5.4 V (two 25 F supercapacitor with rate voltage of 2.7 V in series) using the solar energy harvester with the MPPT circuit. The supercapacitor can be charged while the solar panel operates around 3 V under direct sunlight and changes to around 2.5 V when artificial shadow occurs. This verifies that the proposed MPPT circuit can control the solar panel to operate around its MPP under different environmental conditions.

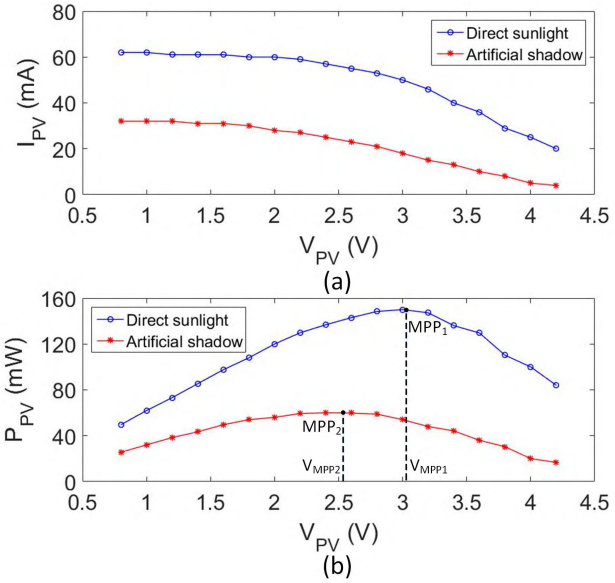

FIGURE 10. I-V (a) and P-V (b) characteristics of the flexible solar panel under the experimental condition.

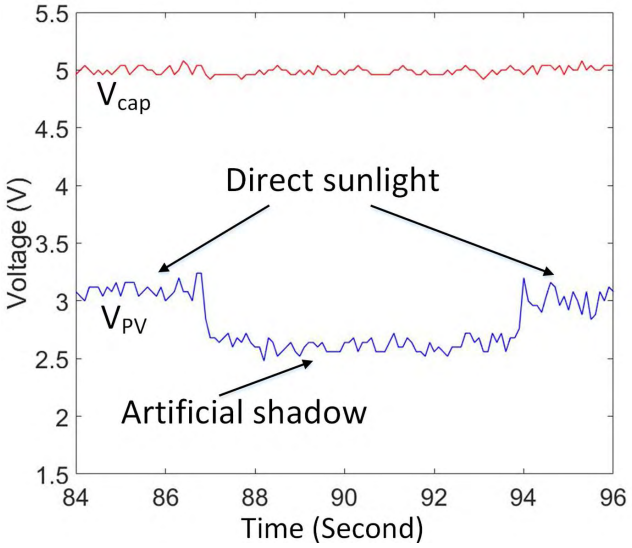

FIGURE 11. Performance of the solar energy harvester with MPPT circuit.

TABLE 1. Time of charging a 12.5 F supercapacitor from 2.4 V to 5.4 V.

Weather condition	Charging time (min)		
	Test1	Test2	Test3
Sunny	25	23	28
Partially cloudy	58	62	65
Cloudy	122	130	115

The solar energy harvester consists of a flexible solar panel, a buck-boost converter, the MPPT circuit and a supercapacitor for energy storage. Table 1 shows the charging performance of the solar energy harvester under different conditions. As the supercapacitors in series have a rate voltage of 5.4 V and the lowest input of the voltage regulator is 2.4 V,

the charging time in Table 1 refers to the time of charging the supercapacitor from 2.4 V to 5.4 V with the proposed solar energy harvester. Experimental results show that the solar energy harvester needs about 30, 60 and 120 min to charge the 12.5 F supercapacitor from 2.4 V to 5.4 V on sunny, partially cloudy and cloudy weather conditions, respectively. In practice, the supercapacitor is charged to 5 V (below the rate voltage) to ensure the long-term behaviour of the supercapacitor.

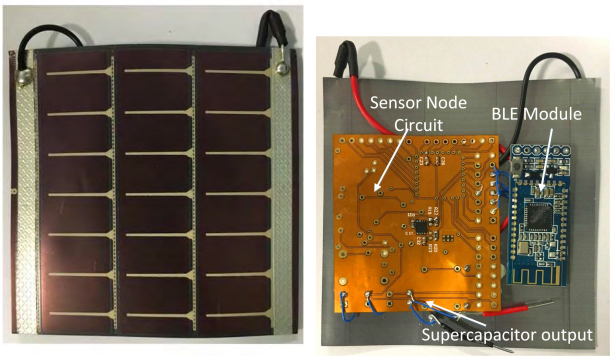

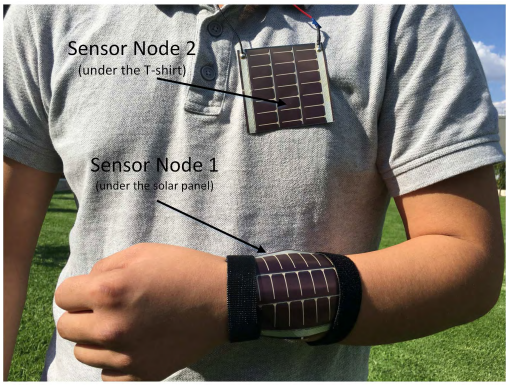

FIGURE 12. The wearable sensor node with solar energy harvesting: (a) front side; (b) back side; (c) experimental setup.

B. WEARABLE SENSOR NODE

Fig. 12 shows the complete setup of the wearable sensor node with the solar energy harvester. Fig. 12(a) illustrates the front side of wearable sensor node, which is the flexible solar panel. The back side consists of the sensor node circuit and the BLE module, which is shown in Fig. 12(b). In the experiment, two wearable sensor nodes are worn by the subject. Sensor Node 1 is on the wrist for the heartbeat and wrist temperature measurement, while Sensor Node 2 is placed on the chest for the body temperature measurement and fall detection, as shown in Fig. 12(c). The data collected from both wearable sensor nodes are transmitted to a smartphone (Fig. 13), which will be monitored by the subject or a healthcare professional. Fig. 13(b) illustrates an example of the realtime plot of the heartbeat and temperature when the subject rides a stationary bicycle for exercise.

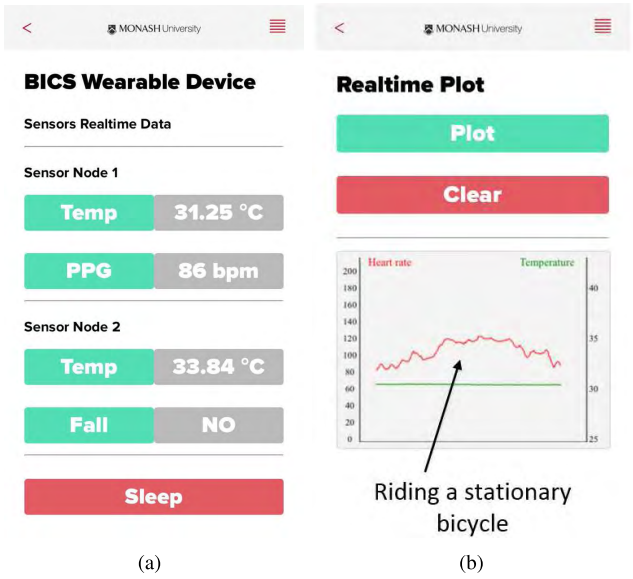

FIGURE 13. The smartphone application for the wearable sensor node: (a) Sensor data from two nodes; (b) The realtime plot of heartbeat and temperature of the wrist node when riding a stationary bicycle.

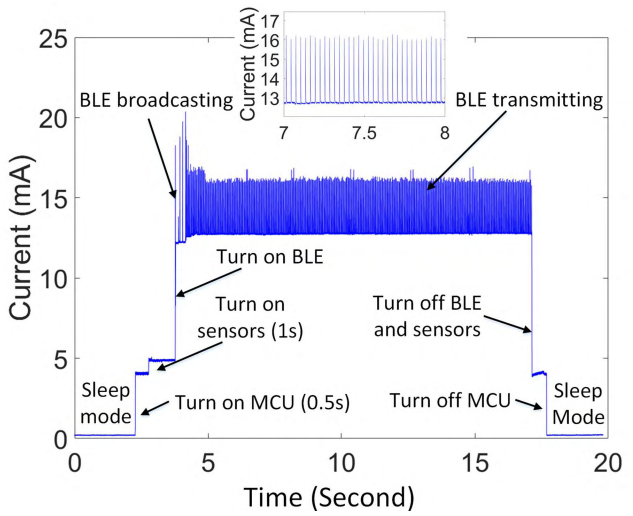

FIGURE 14. Current consumption of the sensor node at different operation stages.

C. ENERGY CONSUMPTION

Low-power consumption is a critical issue in the application of wearable devices as they usually aim for long-term operation. To extend the lifetime of the proposed wearable sensor node, it can be set to sleep mode to save energy when there is no need for a measurement. Fig. 14 illustrates the current consumption of the proposed wearable sensor node during one cycle in the wake-sleep mode. The explicit average currents of the sensor node at different operation stages are presented in Table 2. The operation voltage of the sensor node (V_{node}) is 3.3 V, therefore the average active and sleep energy of the node in one cycle can be calculated as:

$$E_{active} = V_{node} \times (I_1 \times t_1 + I_2 \times t_2 + I_3 \times t_3 + I_4 \times t_4) \quad (7)$$

TABLE 2. The current of the sensor node at different operation stages.

Stage	Mode	Current (mA)	Time (s)
1	MCU (I_1)	4.3	0.5 (t_1)
2	MCU+PPG+ Temperature (I_2)	5.0	1 (t_2)
3	MCU+BLE+PPG+ Temperature (I_3)	14.3	13.5 (t_3)
4	MCU (I_4)	4.3	0.5 (t_4)
5	Sleep (I_5)	0.2	584.5 (t_5)

and

$$E_{sleep} = V_{node} \times I_5 \times t_5 \tag{8}$$

In the experiment the wearable sensor node is set to measure the subject's data every 10 min, which is 14.5 s active mode and 584.5 s sleep mode respectively. Under the experimental configuration the E_{active} is 667.8 mJ and the E_{sleep} is 385.8 mJ, thus the average energy consumption of the wearable sensor node E_{node} is 1053.6 mJ in one 10 min cycle. The corresponding power consumption P_{node} under this operation mode is 1.76 mW (1053.6/600).

D. 24 HOURS OPERATION OF THE WEARABLE SENSOR NODE

To further extend the lifetime of the wearable sensor node or even enable the autonomous 24 hours operation, the solar energy harvester is used to power the sensor node. The energy storage component used is the 12.5 F supercapacitor mentioned previously. Within the normal operation voltage from 2.4 V (lowest input of the voltage regulator) to 5.0 V (below the supercapacitor's rate voltage), the maximum energy stored in the supercapacitor is:

$$\begin{aligned} E_{store} &= \frac{1}{2} \times C \times (V_{max}^2 - V_{min}^2) \\ &= \frac{1}{2} \times 12.5 \times (5.0^2 - 2.4^2) \\ &= 120.25\ J \end{aligned} \tag{9}$$

When the operation cycle of wearable sensor node is set to 10 min, the average energy consumption of the node E_{node} is 1053.6 mJ. The supercapacitor powers the sensor node through a voltage regulator (LTC3130-1), which has a typical efficiency (η_{reg}) of 90% at 3.3 V. By calculation, the fully charged supercapacitor can power the wearable sensor node for:

$$\begin{aligned} N &= \eta_{reg} \times E_{node}/E_{node} \\ &= 90\% \times 120.25/1.0536 \approx 102\ cycles \end{aligned} \tag{10}$$

Therefore the wearable sensor node can be powered by the supercapacitor for 17 hours (102/6) theoretically, which is sufficient for the operation at night. Fig. 15 illustrates the voltage of the supercapacitor in 24 hours. The experiment was done on a sunny day, and the sunrise and sunset time on the experiment date (04/04/2017) is 06:30 am and 18:00 pm

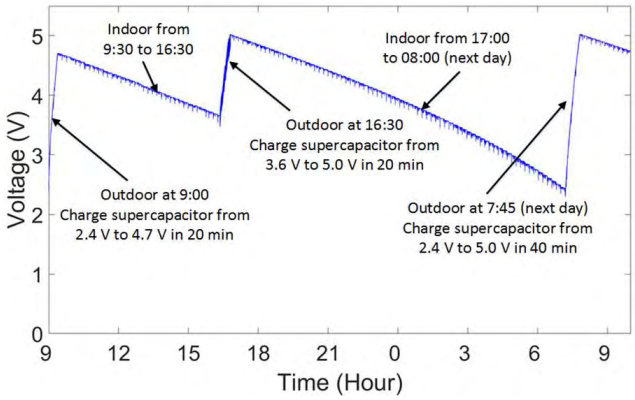

FIGURE 15. 24 hours operation of the wearable sensor node powered by the solar energy harvester.

respectively. The longest operation time of the sensor node achieved is 15 hours (from 17:00 pm to 08:00 am next day). It is less than the theoretical calculation as the supercapacitor has some leakage current. Experimental results demonstrate that the wearable sensor node can autonomously operate 24 hours given that the subject stays outside in the morning and afternoon for 30-60 min to charge the supercapacitor.

V. CONCLUSION AND FUTURE IMPROVEMENT

This paper presents a wearable sensor node with solar energy harvesting that enables the implementation of an autonomous WBAN for IoT connected applications. The proposed wearable sensor nodes can be placed on different positions of the body to measure physical signals like the temperature distribution and heartbeat. It can also detect falls using the accelerometer on the node for emergency notification. In the future, the wearable sensor node can accommodate more signal detections to cover many areas of WBAN applications. A web-based smartphone application is designed to display the sensor nodes' data and send emergency notifications. To extend the lifetime of the wearable sensor node, a solar energy harvester with an output based MPPT technique is used as the power supply. The output based MPPT technique is applied to extract the maximum power from the flexible solar panel. Experimental results show that the wearable sensor node can operate properly when powered by the solar energy harvester. When the sensor node is set to a 10 min wake-sleep mode, the 24 hours operation of the sensor node can be achieved and is verified by experiments. Table 3 summaries some recent wearable WBAN applications with energy harvesting.

The proposed wearable sensor node can be further improved in terms of usability and wearability. For example, the shape of the sensor node can be redesigned to make it more wearable, like a longer but thinner "wrist band". Smart textiles, like bigger flexible solar panels and supercapacitors, can be used to store more energy for the continuous operation of the sensor node. They can be combined with the clothes to make a "smart hat" or "smart T-shirt", so the solar panel can be exposed to more sunlight. The trade-off between

TABLE 3. Comparisons of wearable body area network applications with energy harvesting.

	[17]	[20]	[19]	[21]	This work
Sensors	Temperature	Respiration, heartbeat & accelerometer	Temperature, accelerometer, camera & microphone	Heartbeat & blood pressure	Temperature, heartbeat & accelerometer
Wireless technology	CC2500-2.4 GHz	MAX1472-433 MHz	NFC/RFID	BLE	BLE
Power consumption	3.91 μW	17 mW	Depend on operation mode	41.25 mW	1.76 mW
User interface	PC	PC	EPD	Smartphone	Smartphone
Energy source	flexible solar panel	Flexible Solar panel	8 Solar panels & 7 TEGs	Flexible solar panel	Flexible solar panel
Energy source size (cm^2)	7.2*6	27*17.5	Solar(ea): 3.5*1.4 TEG(ea): 0.8*1	19*4	7.2*6
DC-DC converter	Boost	Buck	Boost with integrated buck	Boost	Buck-boost
MPPT Technique	FOCV	——	FOCV	Indoor: none Outdoor: FLC	Output based MPPT
Energy storage	Supercapacitor 100 mF	Supercapacitor 1 F	Battery 3.7 V 40 mAh	Supercapacitor 500 F	Supercapacitor 12.5 F

the positions of the solar panel for the exposure to sunlight and the positions of the sensor node for the accurate body data measurement will be studied. More sensors for the vital signals of the human body can be integrated with the sensor node, like ECG and EMG. In the future, a secondary battery may also be used as the backup energy storage in case of bad weather conditions.

REFERENCES

[1] G. Fortino and P. Trunfio, *Internet of Things Based On Smart Objects: Technology, Middleware And Applications*. Cham, Switzerland: Springer, 2014.

[2] I. Lee and K. Lee, "The Internet of Things (IoT): Applications, investments, and challenges for enterprises," *Bus. Horizons*, vol. 58, no. 4, pp. 431–440, 2015.

[3] F. Cicirelli, G. Fortino, A. Giordano, A. Guerrieri, G. Spezzano, and A. Vinci, "On the design of smart homes: A framework for activity recognition in home environment," *J. Med. Syst.*, vol. 40, no. 9, pp. 1–17, 2016.

[4] P. Gope and T. Hwang, "BSN-care: A secure IoT-based modern healthcare system using body sensor network," *IEEE Sensors J.*, vol. 16, no. 5, pp. 1368–1376, May 2016.

[5] E. Jovanov and A. Milenkovic, "Body area networks for ubiquitous healthcare applications: Opportunities and challenges," *J. Med. Syst.*, vol. 35, no. 5, pp. 1245–1254, 2011.

[6] R. Gravina, P. Alinia, H. Ghasemzadeh, and G. Fortino, "Multi-sensor fusion in body sensor networks: State-of-the-art and research challenges," *Inf. Fusion*, vol. 35, pp. 68–80, 2017.

[7] C. C. Poon, B. P. Lo, M. R. Yuce, A. Alomainy, and Y. Hao, "Body sensor networks: In the era of big data and beyond," *IEEE Rev. Biomed. Eng.*, vol. 8, no. 1, pp. 4–16, Apr. 2015. [Online]. Available: http://ieeexplore.ieee.org/abstract/document/7096962/

[8] M. R. Yuce, "Implementation of wireless body area networks for healthcare systems," *Sens. Actuators A, Phys.*, vol. 162, no. 1, pp. 116–129, 2010.

[9] G. Fortino, G. Di Fatta, M. Pathan, and A. V. Vasilakos, "Cloud-assisted body area networks: State-of-the-art and future challenges," *Wireless Netw.*, vol. 20, no. 7, pp. 1925–1938, 2014.

[10] G. Aloi *et al.*, "Enabling IoT interoperability through opportunistic smartphone-based mobile gateways," *J. Netw. Comput. Appl.*, vol. 81, pp. 74–84, Mar. 2017.

[11] M. M. Hassan, K. Lin, X. Yue, and J. Wan, "A multimedia healthcare data sharing approach through cloud-based body area network," *Future Generat. Comput. Syst.*, vol. 66, pp. 48–58, Jan. 2017.

[12] K. Sonoda *et al.*, "Wearable photoplethysmographic sensor system with PSOC microcontroller," *Int. J. Intell. Comput. Med. Sci. Image Process.*, vol. 5, no. 1, pp. 45–55, 2013.

[13] Y. H. Kwak, W. Kim, K. B. Park, K. Kim, and S. Seo, "Flexible heartbeat sensor for wearable device," *Biosens. Bioelectron.*, vol. 94, pp. 250–255, Aug. 2017.

[14] C. Vogt *et al.*, "A wearable bluetooth le sensor for patient monitoring during mri scans," in *Proc. 38th Annu. Int. Conf. Eng. Med. Biol. Soc. (EMBC)*, 2016, pp. 4975–4978.

[15] C. Seeger, K. van Laerhoven, and A. Buchmann, "MyHealthAssistant: An event-driven middleware for multiple medical applications on a smartphone-mediated body sensor network," *IEEE J. Biomed. Health Informat.*, vol. 19, no. 2, pp. 752–760, Mar. 2015.

[16] T. J. Voss, V. Subbian, and F. R. Beyette, "Feasibility of energy harvesting techniques for wearable medical devices," in *Proc. 36th Annu. Int. Conf. IEEE Eng. Med. Biol. Soc. (EMBC)*, Aug. 2014, pp. 626–629.

[17] W. Y. Toh, Y. K. Tan, W. S. Koh, and L. Siek, "Autonomous wearable sensor nodes with flexible energy harvesting," *IEEE Sensors J.*, vol. 14, no. 7, pp. 2299–2306, Jul. 2014.

[18] R. Hamid and M. R. Yuce, "A wearable energy harvester unit using piezoelectricŰelectromagnetic hybrid technique," *Sens. Actuators A, Phys.*, vol. 257, pp. 198–207, Apr. 2017.

[19] M. Magno *et al.*, "InfiniTime: Multi-sensor wearable bracelet with human body harvesting," *Sustain. Comput., Inf. Syst.*, vol. 11, pp. 38–49, Sep. 2016.

[20] A. Dionisi, D. Marioli, E. Sardini, and M. Serpelloni, "Autonomous wearable system for vital signs measurement with energy-harvesting module," *IEEE Trans. Instrum. Meas.*, vol. 65, no. 6, pp. 1423–1434, Jun. 2016.

[21] T. V. Tran and W.-Y. Chung, "High-efficient energy harvester with flexible solar panel for a wearable sensor device," *IEEE Sensors J.*, vol. 16, no. 24, pp. 9021–9028, Dec. 2016.

[22] T. Wu, M. S. Arefin, J.-M. Redoute, and M. R. Yuce, "A solar energy harvester with an improved mppt circuit for wearable iot," in *Proc. 11th EAI Int. Conf. Body Area Netw. (Bodynets)*, Turin, Italy, 2016, pp. 166–170.

[23] F. Wu, C. Rüdiger, and M. R. Yuce, "Real-time performance of a self-powered environmental iot sensor network system," *Sensors*, vol. 17, no. 2, pp. 1–14, 2017.

[24] D. Sera, R. Teodorescu, and P. Rodriguez, "PV panel model based on datasheet values," in *Proc. IEEE Int. Symp. Ind. Electron. (ISIE)*, Jun. 2007, pp. 2392–2396.
[25] P. Bhatnagar and R. Nema, "Maximum power point tracking control techniques: State-of-the-art in photovoltaic applications," *Renew. Sustain. Energy Rev.*, vol. 23, pp. 224–241, Jul. 2013.
[26] S. E. Babaa, M. Armstrong, and V. Pickert, "Overview of maximum power point tracking control methods for PV systems," *J. Power Energy Eng.*, vol. 2, no. 8, 2014, Art. no. 49283.
[27] N. Femia, G. Petrone, G. Spagnuolo, and M. Vitelli, "A technique for improving P&O MPPT performances of double-stage grid-connected photovoltaic systems," *IEEE Trans. Ind. Electron.*, vol. 56, no. 11, pp. 4473–4482, Nov. 2009.
[28] Y. Wang *et al.*, "Storage-less and converter-less photovoltaic energy harvesting with maximum power point tracking for Internet of Things," *IEEE Trans. Comput.-Aided Design Integr.*, vol. 35, no. 2, pp. 173–186, Feb. 2016.
[29] A. Frezzetti, S. Manfredi, and A. Suardi, "Adaptive FOCV-based control scheme to improve the mpp tracking performance: An experimental validation," *IFAC Proc. Vols.*, vol. 47, no. 3, pp. 4967–4971, 2014.
[30] T. Wu, M. S. Arefin, D. Shmilovitz, J.-M. Redoute, and M. R. Yuce, "A flexible and wearable energy harvester with an efficient and fast-converging analog MPPT," in *Proc. 12th Biomed. Circuits Syst. Conf. (BioCAS)*, 2016, pp. 336–339.

TAIYANG WU (S'16) received the B.E. degree from Southeast University, Nanjing, China, in 2014. He is currently pursuing the Ph.D. degree in electrical and computer systems engineering with Monash University. His main areas of research interest are energy harvesting, wireless sensor network, and IoT connected applications.

FAN WU (S'17) received the B.E. degree from Monash University in 2015, where he is currently pursuing the Ph.D. degree in electrical and computer systems engineering. He was a Research Assistant with the Engineering Department from 2015 to 2017. His main areas of research interest are wireless sensor network, energy harvesting, and IoT innovations.

JEAN-MICHEL REDOUTÉ (M'09–SM'12) received the M.S. degree in electronics from the University College of Antwerp, Belgium, in 1998, the M.Eng. degree in electrical engineering from the University of Brussels, Belgium, in 2001, and the Ph.D. degree from the University of Leuven in 2009. His Ph.D. entitled Design of EMI resisting analog integrated circuits. In 2001, he was with Alcatel Bell, Antwerp, where he was involved in the design of analog microelectronic circuits for telecommunications systems. In 2005, he joined ESAT-MICAS Laboratories, University of Leuven, as a Ph.D. Research Assistant. In 2009, he was with the Berkeley Wireless Research Center, University of California at Berkeley, as a Post-Doctoral Scholar. In 2010, he joined Monash University as a Senior Lecturer. His research interests include mixed-signal integrated circuit design, electromagnetic compatibility, biomedical (integrated and non-integrated) circuit design, and radio-frequency integrated circuit design.

MEHMET RASIT YUCE (S'01–M'05–SM'10) received the M.S. degree in electrical and computer engineering from the University of Florida, Gainesville, FL, in 2001, and the Ph.D. degree in electrical and computer engineering from North Carolina State University, Raleigh, NC, in 2004. He was a Post-Doctoral Researcher with the Electrical Engineering Department, University of California at Santa Cruz, in 2005. He was an Academic Member with the School of Electrical Engineering and Computer Science, University of Newcastle, NSW, Australia, until 2011. In 2011, he joined Monash University, Australia, where he is currently an Associate Professor with the Department of Electrical and Computer Systems Engineering. He has authored over books *Wireless Body Area Networks* published in 2011 and *Ultra-Wideband and 60 GHz Communications for Biomedical Applications* published in 2013. His research interests include wearable devices, Internet-of-Things for healthcare, wireless implantable telemetry, wireless body area network, bio-sensors, and integrated circuit technology dealing with digital, analog, and radio frequency circuit designs for wireless, biomedical, and RF applications. He has authored over 150 technical articles in the above areas and received the NASA Group Achievement Award in 2007 for developing an SOI transceiver. He received the Best Journal Paper Award in 2014 from the IEEE Microwave Theory and Techniques Society. He received the Research Excellence Award in the Faculty of Engineering and Built Environment, University of Newcastle, in 2010. He is a Topical Editor of the IEEE Sensors Journal and a Guest Editor of the IEEE Journal of Biomedical and Health Informatics in 2015.